THE JOURNAL OF BIOLOGICAL CHEMISTRY VOL. 287, NO. 3, pp. 1823–1836, January 13, 2012

Insulin Protects Pancreatic Acinar Cells from Cytosolic Calcium Overload and Inhibition of Plasma Membrane Calcium Pump*

Received for publication, November 22, 2011, and in revised form, November 29, 2011 Published, JBC Papers in Press, November 29, 2011, DOI 10.1074/jbc.M111.326272

Parini Mankad[‡1], **Andrew James**[‡], **Ajith K. Siriwardena**[§], **Austin C. Elliott**[‡], **and Jason I. E. Bruce**[‡2]

From the [‡]*Faculty of Life Sciences, The University of Manchester and the* [§]*Hepatobiliary Surgery Unit, Manchester Royal Infirmary, Manchester M13 9NT, United Kingdom*

Background: Impaired metabolism and cytosolic Ca^{2+} overload in pancreatic acinar cells can trigger pancreatitis.
Results: Insulin protected cells from oxidant-induced Ca^{2+} overload, inhibition of the plasma membrane calcium pump (PMCA), and ATP depletion.
Conclusion: Insulin switches metabolism toward glycolysis and fuels the PMCA even when mitochondria are impaired.
Significance: This mechanism may provide an important therapeutic strategy for pancreatitis.

Acute pancreatitis is a serious and sometimes fatal inflammatory disease of the pancreas without any reliable treatment or imminent cure. In recent years, impaired metabolism and cytosolic Ca^{2+} ($[Ca^{2+}]_i$) overload in pancreatic acinar cells have been implicated as the cardinal pathological events common to most forms of pancreatitis, regardless of the precise causative factor. Therefore, restoration of metabolism and protection against cytosolic Ca^{2+} overload likely represent key therapeutic untapped strategies for the treatment of this disease. The plasma membrane Ca^{2+}-ATPase (PMCA) provides a final common path for cells to "defend" $[Ca^{2+}]_i$ during cellular injury. In this paper, we use fluorescence imaging to show for the first time that insulin treatment, which is protective in animal models and clinical studies of human pancreatitis, directly protects pancreatic acinar cells from oxidant-induced cytosolic Ca^{2+} overload and inhibition of the PMCA. This protection was independent of oxidative stress or mitochondrial membrane potential but appeared to involve the activation of Akt and an acute metabolic switch from mitochondrial to predominantly glycolytic metabolism. This switch to glycolysis appeared to be sufficient to maintain cellular ATP and thus PMCA activity, thereby preventing Ca^{2+} overload, even in the face of impaired mitochondrial function.

Acute pancreatitis is an inflammatory disease of the pancreas with an incidence of 1 in 10,000 and an overall disease-related mortality of 5%, which is considerably higher (17%) in severe necrotic disease (1). One-third of patients develop severe disease with in-patient stays of up to 100 days. There is no specific intervention for acute pancreatitis, and it is clear that the current paradigms of understanding of the disease are inadequate. Although the underlying pathology is poorly understood, acute pancreatitis is often characterized by the autodigestion of the exocrine tissue, caused either by impaired Ca^{2+}-dependent exocytosis of digestive enzymes or by intracellular enzyme activation (1, 2). This leads to a spiral of self-perpetuating necrotic tissue damage and a consequent local, and then systemic, inflammatory response. In severe cases this can lead to distal organ damage, multiple organ failure, and death (1).

There are several diverse causative factors for pancreatitis, including bile acid reflux from gall stones or biliary disease, ethanol metabolites from excessive alcohol intake, hypertriglyceridaemia, and oxidative stress (1, 2). However, over the last several years, these causative factors have each been shown to impair the normal cytosolic Ca^{2+} concentration ($[Ca^{2+}]_i$) homeostasis and $[Ca^{2+}]_i$ signaling in pancreatic acinar cells (2). In particular, an irreversible increase in $[Ca^{2+}]_i$ (Ca^{2+} overload) has been suggested to be a key feature of acute pancreatitis, regardless of the causative agent or process. Oxidative stress has also been implicated in pancreatitis, either as a cellular trigger (3) or in facilitating the inflammatory response (4).

We have previously reported that oxidative stress, induced by H_2O_2, profoundly altered hormone-evoked $[Ca^{2+}]_i$ signaling and resulted in an irreversible Ca^{2+} overload and a marked inhibition of the plasma membrane Ca^{2+}-ATPase (PMCA)[3] in pancreatic acinar cells (5, 6). Although oxidative stress can affect many Ca^{2+} transport/signaling pathways, the PMCA has an especially key role as the final "gatekeeper" for the control of resting $[Ca^{2+}]_i$, especially in cells in which the Na^+-Ca^{2+} exchange is not expressed (7). Even when all other Ca^{2+} transport pathways are impaired, $[Ca^{2+}]_i$ will recover close to resting

* This work was supported by a Biotechnology and Biological Sciences Research Council New Investigator Grant (to J. I. E. B.) and a Central Manchester Foundation Trust/National Institutes of Health Research Manchester Biological Research Centre pump priming fund (to A. K. S. and J. I. E. B.). Preliminary accounts of these data have been presented at meetings of the Physiological Society and American Pancreatic Association.
[1] Supported by a Biotechnology and Biological Sciences Research Council Ph.D. studentship.
[2] To whom correspondence should be addressed: Faculty of Life Sciences, The University of Manchester, Michael Smith Building, Oxford Road, Manchester M13 9NT, UK. Tel: + 44–161-275–5484; Fax: +44–161-275–5600. Email Address: jason.bruce@manchester.ac.uk

[3] The abbreviations used are: PMCA, plasma membrane Ca^{2+}-ATPase; DCF, dichlorofluorescein; TMRM, tetramethylrhodamine methylester; CCCP, carbonylcyanide *m*-chlorophenylhydrazone; AUC, area under the curve; mPTP, mitochondrial permeability transition pore; IOA, iodoacetate; BrPyr, 3-bromopyruvate; CCK cholecystokinin; PSS, physiological saline solution; TRITC, tetramethylrhodamine isothiocyanate; MgGreen, magnesium green.

levels as long as the PMCA remains active or "protected" (8). This will allow cells to recover from potential insults that raise $[Ca^{2+}]_i$ by activating the necessary stress response pathways or even triggering the "safe" dismantling of the cell constituents by apoptosis or autophagy (9). However, if the PMCA becomes inhibited, excess Ca^{2+} in the cytosol cannot be exported, and $[Ca^{2+}]_i$ will remain high, leading to catastrophic necrotic cell death. Therefore, understanding the mechanism for this inhibition of the PMCA and/or mechanisms by which the PMCA can be protected could be an important basis for therapeutic strategies for acute pancreatitis, regardless of the precise causative factor or process.

Insulin, which is endogenously released from pancreatic β-cells adjacent to pancreatic acinar cells within the pancreas, has been reported to protect against pancreatitis, both in experimental animal models (10–13) and in the treatment of the human disease (14–16). For example, in L-arginine-induced experimental models of acute pancreatitis, most pancreatic acinar cells undergo damage, but acinar cells surrounding the islets of Langerhans remain relatively intact (10, 11). This periinsular (or peri-islet) acinar cell protection was abolished in streptozotocin-induced diabetic rats, where insulin secretion is impaired (10, 11). Moreover, regeneration of exocrine pancreatic tissue was abolished in diabetic rats and restored following the administration of exogenous insulin (11–13). In addition, several related growth factors/gastrointestinal peptides that couple to similar signaling pathways to insulin (*e.g.* PI3K/Akt) have also been shown to be protective in several models of pancreatitis (17–19). Finally, activation of PI3K/Akt signaling pathways has been extensively reported to protect a variety of cells from oxidative injury, activate pro-survival pathways, and inhibit cell death pathways (20–22). The aim of the current study was therefore to test the protective effects of insulin on oxidant-mediated impairment of Ca^{2+} signaling and inhibition of the PMCA. The results show that insulin protects against the oxidant-induced Ca^{2+} overload and inhibition of the PMCA in a PI3K-dependent manner that correlated with Akt phosphorylation. Insulin had no effect on H_2O_2-induced oxidative stress or mitochondrial depolarization but appeared to reduce relative mitochondrial NADH production and enhance relative glycolytic NADH production. Insulin also attenuated the oxidant-induced ATP depletion, suggesting that this metabolic switch toward glycolysis was sufficient to maintain ATP. Moreover, insulin potentiated the inhibition of the PMCA by glycolytic inhibitors and abolished inhibition of the PMCA by mitochondrial inhibitors. This suggests that insulin may protect pancreatic acinar cells by switching from mitochondrial to predominantly glycolytic metabolism as the major ATP fuel for the PMCA, thereby maintaining low resting $[Ca^{2+}]$ in the face of impaired mitochondrial function.

EXPERIMENTAL PROCEDURES

Cell Isolation—Pancreatic acinar cells from Sprague-Dawley rats were isolated by collagenase digestion as previously described (5, 6). For all of the fluorescence imaging experiments, the cells were perfused with a HEPES-buffered physiological saline solution (HEPES-PSS; 137 mM Na^+, 4.7 mM K^+, 0.56 mM Mg^{2+}, 1.28 mM Ca^{2+}, 145.34 mM Cl^-, 10 mM HEPES, 5.5 mM glucose, pH 7.4). All of the drug solutions were made up from frozen stocks immediately prior to use.

Imaging of Fura-2 Fluorescence—Pancreatic acinar cells were loaded with 4 μM fura-2-AM (Invitrogen) for 30 min at room temperature in HEPES-PSS as previously described (5). Fura-2-loaded cells were imaged using an identical microscope/imaging system to previous studies (5), and fura-2 fluorescence was calibrated into "estimated" $[Ca^{2+}]_i$ as previously described (6). All of the experiments were carried out at room temperature (20–22 °C).

Imaging of Dichlorofluoroscein (DCF) Fluorescence—Cellular oxidative stress was assessed using the fluorescent dye DCF, similar to our previous study (6). Pancreatic acinar cells were loaded with the nonfluorescent dichlorodihydrofluoroscein diacetate (Invitrogen) at 10 μM for 30 min at room temperature. The cells were excited with light at 488 nm ($\pm$ 10 nm), and the background-subtracted images were captured every 10 s through a fluoroscein dichroic (510 nm; Chroma) with 5 $\times$ 5 binning. The relative increase in DCF fluorescence was expressed as F/F_0 (where F_0 was the average initial fluorescence) and normalized to an extrapolated baseline following treatment with H_2O_2, with or without insulin.

Measurement of Mitochondrial Membrane Potential ($\Delta\Psi m$)—Mitochondrial membrane potential ($\Delta\Psi m$) was determined using the fluorescent dye tetramethylrhodamine methylester (TMRM), as previously described (5). Pancreatic acinar cells were loaded with 100 nM TMRM for 15 min at 37 °C, and all of the perfusion solutions thereafter also contained 100 nM TMRM to minimize dye leakage. TMRM-loaded cells were excited with 545 $\pm$ 10-nm excitation light (50-ms exposure) and emitted fluorescence was captured through a TRITC dichroic (Chroma) every 5 s. Changes in relative TMRM fluorescence within mitochondrial regions were expressed as F/F_0. The effect of H_2O_2 on mitochondrial membrane potential was further normalized by expressing changes in F/F_0 as a percentage of the maximum depolarization evoked by the uncoupler CCCP.

Western Blotting—Viable pancreatic acinar cells were separated from nonviable cells using Optiprep™ density gradient medium (Axis Shield Dundee, UK). Acinar cell suspension was layered onto Optiprep™ at a density of 1.018 g ml^{-1} and centrifuged at 800 $\times$ *g* for 17 min at 4 °C. The pellet containing nonviable cells was discarded, and the viable cells were washed in HEPES-PSS and resuspended in 1% BSA. The cells were then treated with or without (control) test reagents (*e.g.* 100 nM insulin and/or 10 μM LY294002). Following treatment, the cells were lysed in radioimmune precipitation assay buffer, sonicated, and left to solubilize for 30 min on ice. Radioimmune precipitation assay buffer contained 12 mM HEPES, 300 mM mannitol, 1 mM EDTA, 1 mM EGTA, 0.1 mM vanadate, 1 mM NaF, 0.25 mM $Na_4P_2O_7$, 1% Triton X-100, 0.1% SDS, and an EDTA-free protease inhibitor tablet (Roche Applied Science). The lysates were then centrifuged at 300 $\times$ *g* for 15 min, and the supernatant was transferred into a fresh, ice-cold Eppendorf tube. Sample buffer containing β-mercaptoethanol was added at ⅓ supernatant volume, and the mixture was boiled at 95 °C for 5 min. The proteins were separated using SDS-PAGE and transferred onto a nitrocellulose membrane. The membranes

were then blocked in 5% BSA for 1 h at room temperature. Following this, the membranes were then washed and blotted with primary antibody (rabbit monoclonal anti-phospho-AktS473 or pan Akt antibody; Cell Signaling) at 4 °C in 5% BSA either for 2 h or overnight. The membranes were again washed and then probed with anti-rabbit secondary antibody for 1 h at room temperature. Following a final wash, the membranes were incubated in ECL for 3 min and then exposed to x-ray film and developed.

Imaging of NADH Autofluorescence—Pancreatic acinar cells were excited with light at 350 nm (500-ms exposure), and NADH autofluorescence was collected through a fura-2 400-nm dichroic filter without a band pass filter. Sequential background-subtracted images were acquired every 5 s, and changes in NADH autofluorescence were quantified as raw fluorescence gray levels. To determine the relative mitochondrial and glycolytic contributions to NADH autofluorescence, the cells were treated with 4 μM CCCP and then 2 mM iodoacetate (IAA), respectively.

Measurement of Cellular ATP—ATP depletion in response to H_2O_2 (with or without insulin) was determined using two complimentary techniques. These were the Mg^{2+}-sensitive fluorescent dye, magnesium green (MgGreen) used in intact living cells and an *in vitro* chemiluminescence assay of firefly luciferase using cell extracts (ViaLight® Plus kit, Lonza, Rockland, ME, UK). MgGreen senses free $[Mg^{2+}]_i$ at concentrations around the resting $[Mg^{2+}]_i$ (~0.9 mM) and was thus used as an indirect measure of cytosolic ATP depletion, similar to our previous study (5). This is because most cytosolic ATP exists as MgATP, and ATP depletion therefore increases free $[Mg^{2+}]_i$ and thus MgGreen fluorescence. Pancreatic acinar cells were incubated with 4 μM MgGreen for 30 min at room temperature and excited with 496 ± 10-nm excitation light (50 ms exposure) every 10 s. Background-subtracted images were captured using 5 × 5 binning through a FITC dichroic (Chroma). Fluorescent signals were expressed as relative fluorescence normalized to fluorescence from the initial 10 frames (F/F_0). The cells were treated with or without 100 nM insulin for 20 min, followed by 500 μM H_2O_2 for a further 20 min before treatment with an ATP depletion mixture (4 μM CCCP, 500 μM bromopyruvate, 10 μM oligomycin, 2 mM iodoacetate, and 100 μM carbachol) for a final 20 min to induce maximum ATP depletion. All of the responses to H_2O_2 were normalized to the maximum ATP depletion following treatment with the ATP depletion mixture, similar to our previous experiments.

The *in vitro* ViaLight® Plus kit (Lonza, Rockland, ME, UK) was also used to assess cellular ATP. This measures the luminescence emitted from the firefly luciferase-catalyzed ATP-dependent oxidation of luciferin, using a luminescence multiplate reader (BioTEK Synergy HT). The kit was used according to the manufacturer's instructions, with minor modifications because of the use of acutely isolated, rather than cultured, cells. Pancreatic acinar cells were treated with HEPES-PSS with or without 100 nM insulin for 20 min, followed by treatment with or without various concentrations of H_2O_2 (0–1 mM) for a further 20 min before treatment with or without the ATP depletion mixture (for 20 min). The cells were aliquoted into Eppendorf tubes and centrifuged between the above sequential treatments, prior to the final resuspension in 100 μl of cell lysis reagent for 10 min. Each cell lysate was added to 100 μl of ATP Monitoring Reagent Plus in a 96-well plate and left for 2 min prior to measuring the luminescence. All of the experimental treatment regimes were performed in parallel within the same experiment (*i.e.* on the same cell preparation), and all of the tubes were centrifuged at the same time to avoid the loss of cells during centrifugation from influencing the results. Each experiment also contained a time-matched control, in which cells received no drug treatment, but were centrifuged at the equivalent time points, and thus represent total ATP. Finally, for ATP depletion, each experiment also contained a positive control in which an equal aliquot of cells was treated with the ATP depletion mixture (during the final 20 min), which thus represented maximal/total ATP depletion. The total luminescence count of the ATP depletion mixture (maximum ATP depletion) was subtracted from the luminescence count from each corresponding assay condition prior to normalization to the corresponding time-matched control (%) in each experimental run.

Data Analysis and Experimental Design—Changes in resting $[Ca^{2+}]_i$ were quantified using both the maximum increase in $[Ca^{2+}]_i$ (magnitude) and area under the curve (AUC) and responses compared using an unpaired Student's *t* test. For $[Ca^{2+}]_i$ clearance experiments, a paired experimental design was adopted, in which two repeated Ca^{2+} clearance phases were elicited, and the normalized linear $[Ca^{2+}]_i$ clearance rate was compared with time-matched control experiments using a Mann-Whitney test (5). For TMRM experiments, the responses were normalized to the CCCP response and compared using a Mann-Whitney test. For each experimental maneuver there was a minimum of four separate experiments performed, each containing 5–20 cells. For any given parameter analyzed, an "experimental average response" was determined from all of the cells (5–20) in a particular experiment. These values were in turn averaged to give the true overall mean ± S.E.

RESULTS

Insulin Protects Against H_2O_2-induced Ca^{2+} Overload—In the present study, we have tested the putative protective effect of insulin on the H_2O_2-induced Ca^{2+} overload response in pancreatic acinar cells. The nature of the experimental design and analytical methods are described in more detail in our previous work (5). Pancreatic acinar cells were pretreated with or without 100 nM insulin for 30 min, because this concentration is known to cause maximum activation of glucose uptake in insulin-responsive tissues such as skeletal muscle and adipocytes (23–25). The cells were then treated with 100 μM H_2O_2 (which approximates the EC_{50} value for H_2O_2 (6)) for 10 min followed by a further recovery period of 10 min. These experiments were repeated with or without 30 min of pretreatment with 100 nM insulin (Fig. 1). Responses were quantified by measuring both the maximum H_2O_2-induced change in resting $[Ca^{2+}]_i$ (max Δ Ca^{2+}; Fig. 1*D*) and the AUC (Fig. 1*E*) for the $[Ca^{2+}]_i$ response. The AUC reflects both the magnitude *and* any recovery of the response and was therefore measured over a 20-min period that consisted of 10 min of H_2O_2 treatment and 10 min of recovery (Fig. 1).

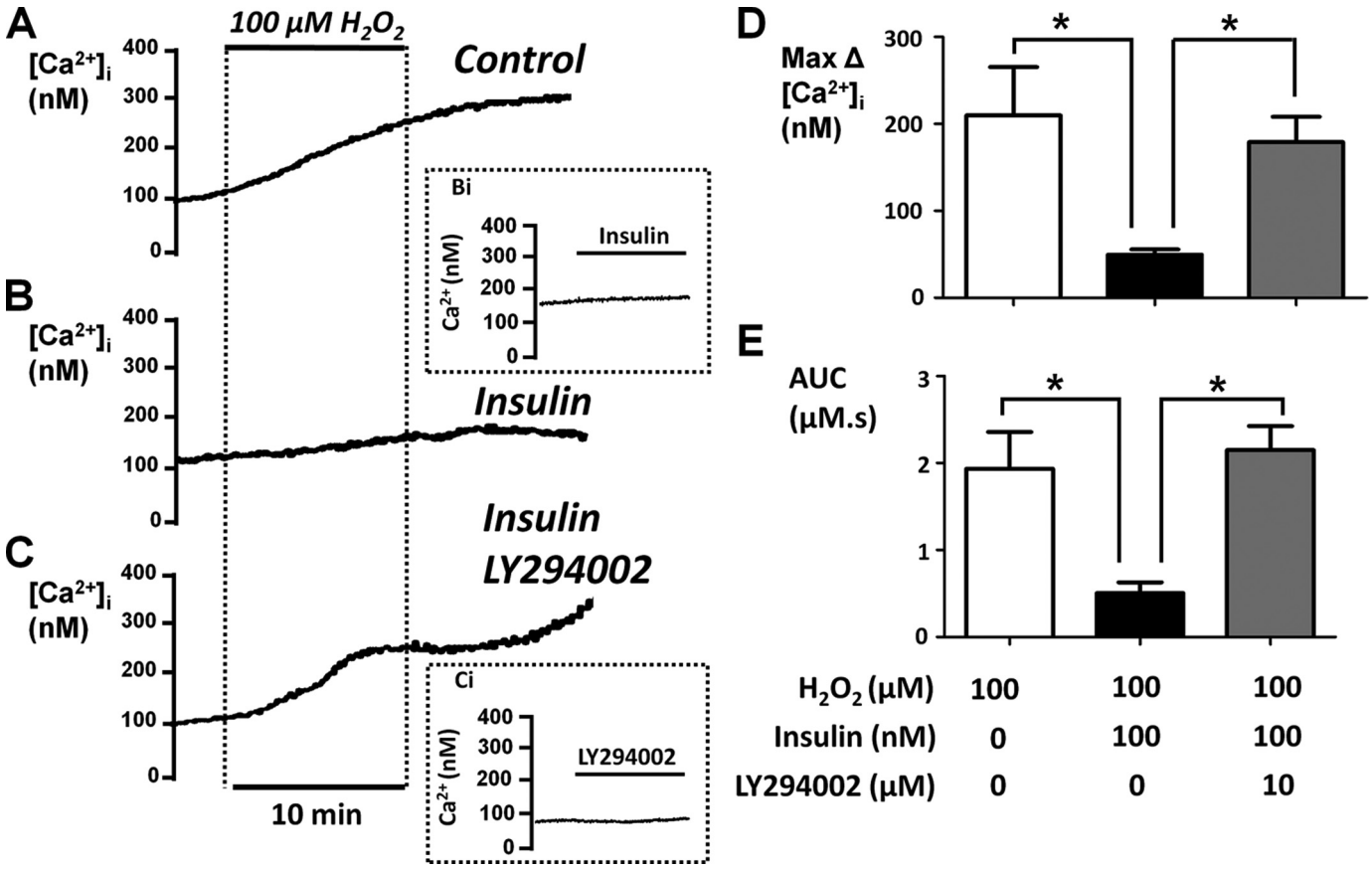

FIGURE 1. **Insulin protects the H_2O_2-induced Ca^{2+} overload in a PI3K-dependent manner.** Fura-2-loaded pancreatic acinar cells were treated with 100 μM H_2O_2 for 10 min where indicated. The cells were either untreated (*Control*, $n = 15$; *A*) or pretreated with 100 nM insulin (*Insulin*, $n = 9$; *B*) or a combination of insulin and the PI3K inhibitor LY294002 (10 μM) (*Insulin LY294002*, $n = 15$; *C*) for 30 min prior to the addition of H_2O_2. The mean data (± S.E.) are shown for the maximum H_2O_2-induced change in resting $[Ca^{2+}]_i$ (*Max* $\Delta[Ca^{2+}]_i$; *D*) and AUC (*E*) over the treatment and recovery period. *, $p < 0.05$ as determined by unpaired Student's *t* test.

On average, 100 μM H_2O_2 increased $[Ca^{2+}]_i$ by 235 ± 57 nM ($n = 15$), which was reduced to 54 ± 6 nM ($n = 9$, $p < 0.05$ *versus* control cells) in the presence of insulin. Likewise, the H_2O_2-induced increase in the AUC (2.05 ± 0.4 μM·s, $n = 15$) was also markedly attenuated in insulin-treated cells (0.55 ± 0.1 μM·s, $n = 7$, $p < 0.05$). When applied to pancreatic acinar cells alone, insulin (100 nM to 10 μM) had no direct effect on resting $[Ca^{2+}]_i$ (Fig. 1, *inset Bi*), suggesting that even at higher concentrations, insulin does not cause cytotoxicity over this time scale.

Insulin Protection against H_2O_2-induced Ca^{2+} Overload Is Prevented by LY294002—To test whether the protective effects of insulin were due to activation of PI3K/Akt pathways, the cells were treated with the PI3K inhibitor LY294002 (10 μM). When applied alone, LY294002 had no effect on resting $[Ca^{2+}]_i$ (Fig. 1, *inset Ci*), suggesting that inhibition of any constitutively active PI3K has no effect on resting $[Ca^{2+}]_i$. However, the combined treatment of cells with LY294002 (10 μM) and insulin (100 nM) abolished the protective effect of insulin (Fig. 1, *C–E*).

Insulin Has No Effect on H_2O_2-induced Oxidative Stress—Cells exhibited minimal fluorescence until treated with H_2O_2, which oxidized the nonfluorescent dichlorodihydrofluorescein to the fluorescent DCF. In some cells there was a slight upwards drift in DCF fluorescence, probably because of endogenous cellular oxidant production. The change in relative fluorescence (F/F_0) induced by H_2O_2 was therefore calculated from an extrapolated linear baseline. H_2O_2 (0.1–1 mM) caused a concentration-dependent increase in relative DCF fluorescence (0.1 mM H_2O_2: $\Delta F/F_0 = 19 \pm 4\%$ ($n = 4$), $p < 0.05$; 0.5 mM: $\Delta F/F_0 = 32 \pm 10\%$ ($n = 6$), $p < 0.05$; 1 mM: $\Delta F/F_0 = 31 \pm 6\%$ ($n = 8$), $p < 0.05$; Fig. 2, *A* and *C*). Pretreatment of cells with 100 nM insulin for 30 min had no significant effect on the H_2O_2-induced increase in oxidative stress (0.1 mM: 10 ± 2% ($n = 3$); 0.5 mM: 35 ± 5% ($n = 6$); 1 mM: 24 ± 6% ($n = 8$); Fig. 2, *B* and *C*). When applied alone, 100 nM insulin had no effect on DCF fluorescence (data not shown). These data suggest that insulin did not protect pancreatic acinar cells by reducing the H_2O_2-induced cellular oxidative stress, for instance by increasing cellular antioxidant capacity.

H_2O_2 Causes a Concentration-dependent Inhibition of the PMCA—To test whether the protective effect of insulin on H_2O_2-induced Ca^{2+} overload was due to protection of PMCA activity, we utilized an *in situ* $[Ca^{2+}]_i$ clearance assay similar to our previous study (5). In essence, this approach controls for both cell-to-cell and time-dependent differences in $[Ca^{2+}]_i$ clearance rate by making repeated measurements of $[Ca^{2+}]_i$ clearance, in parallel, on cells from the same experimental animal. This then allows changes in clearance/PMCA activity caused by experimental treatments (H_2O_2, insulin, LY294002) to be clearly identified. The cells were treated with cyclopi-

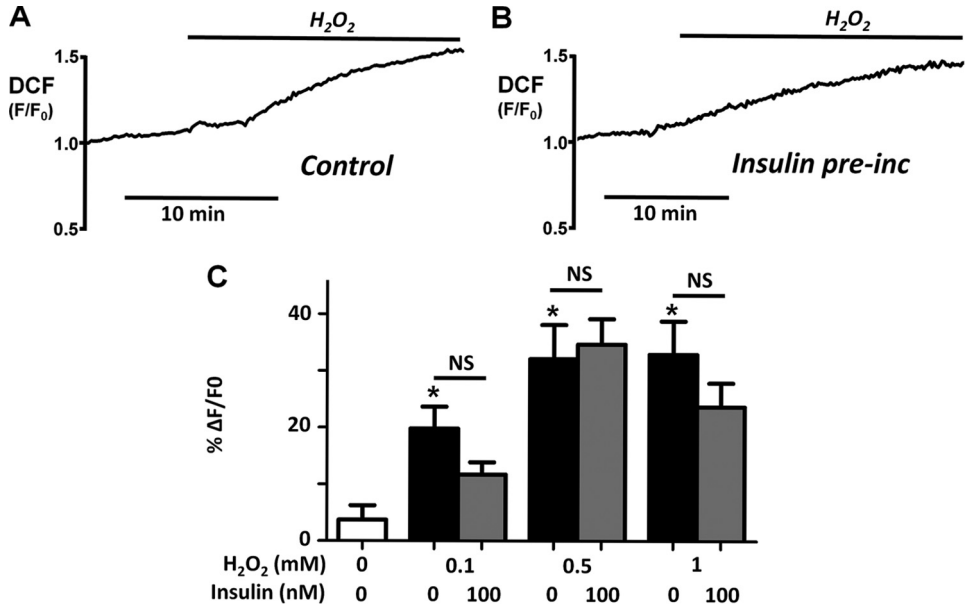

FIGURE 2. **Insulin has no effect on H_2O_2-induced oxidative stress.** *A* and *B*, representative traces showing the relative DCF fluorescence (F/F_0) in response to 500 μM H_2O_2 in untreated control pancreatic acinar cells (*A*) or following pretreatment with 100 nM insulin for 30 min (*B*). *C*, overall mean data (± S.E.) showing the change in DCF fluorescence (%$\Delta F/F_0$) in response to 0.1 ($n = 4$), 0.5 ($n = 6$), and 1 mM H_2O_2 ($n = 8$) in the absence (*light gray box*) or presence (*dark gray box*) of 100 nM insulin. * represents statistical significance, $p < 0.05$ by comparing to time-matched control experiments (*white box*) as determined by a nonparametric Mann-Whitney *U* test. *NS* represents not significant when compared between control and insulin-treated cells. *pre-inc*, preincubation.

azonic acid in the absence of external Ca^{2+}; this inhibits the sarco/endoplasmic reticulum Ca^{2+}-ATPase, facilitates the net leak of Ca^{2+} from the ER, and thus slowly depletes the ER of Ca^{2+}. This maneuver causes a slow increase in $[Ca^{2+}]_i$, which slowly recovers to baseline because of Ca^{2+} efflux via the PMCA. Because of the ER Ca^{2+} depletion and the consequent switching on of store-operated Ca^{2+} entry channels, the addition of high external Ca^{2+} (20 mM) to cells under these conditions causes a rapid increase in $[Ca^{2+}]_i$, which reaches a short-lived steady state because of a balance of Ca^{2+} entry and Ca^{2+} efflux. Subsequent removal of external Ca^{2+} (0 Ca^{2+}, 1 mM EGTA) causes a rapid clearance of $[Ca^{2+}]_i$ back to resting values, predominantly because of PMCA activity (Fig. 3). As previously described (5), this $[Ca^{2+}]_i$ clearance can be quantified by either fitting the falling phase to a single exponential decay or by measuring the linear rate from a standardized value of $[Ca^{2+}]_i$ (see our previous study (5)). However, fitting to a single exponential decay becomes unreliable when clearance is inhibited to the extent that only a very slow clearance rate is measurable. Under these circumstances, the rate of clearance is quasi-linear, and therefore the linear rate of clearance was chosen for quantification.

Using this approach, the second clearance rate was found to be on average 92 ± 12% of the initial clearance rate in time-matched control experiments ($n = 8$). Treatment with H_2O_2 caused a concentration-dependent inhibition of this relative $[Ca^{2+}]_i$ clearance rate (50 μM, 46 ± 10%, $n = 4$, $p < 0.05$; 100 μM, 32 ± 6%, $n = 6$, $p < 0.05$; 500 μM, 12 ± 5%, $n = 6$, $p < 0.05$; Fig. 3), in accordance with our previous work (5).

Insulin Protects against H_2O_2-induced Inhibition of the PMCA in a PI3K-dependent Manner—We next tested whether insulin protected this H_2O_2-induced inhibition of the PMCA. A single concentration of 100 μM H_2O_2 was chosen, because this was close to the IC_{50} value for PMCA inhibition (Fig. 3). In insulin-treated cells, 100 μM H_2O_2 reduced $[Ca^{2+}]_i$ clearance to 57 ± 3% (Fig. 4*B*; $n = 6$) of control, demonstrating less inhibition of $[Ca^{2+}]_i$ clearance by H_2O_2 than in untreated control cells (32 ± 6%; Fig. 4*A*; $n = 6$, $p < 0.05$). This suggests that insulin partially protects the PMCA from inhibition by oxidative stress. To test whether this protection was due to activation of the PI3K/Akt pathway, we again incubated cells with the PI3K/Akt inhibitor LY294002 (10 μM) in combination with 100 nM insulin (Fig. 4, *C–E*). This restored the full inhibitory effect of H_2O_2 on $[Ca^{2+}]_i$ clearance (reduced to 30 ± 5% of control, $n = 5$; Fig. 4*E*). These data collectively suggest that insulin protects the PMCA from oxidative stress caused by activation of PI3K pathways.

Insulin Causes a PI3K-dependent Akt Phosphorylation in Pancreatic Acinar Cells—We next verified that treatment of pancreatic acinar cells with insulin activates insulin-dependent PI3K/Akt by Western blotting using the pAktS473 antibody (Fig. 5). This detects the phosphorylated serine residue at position 473 on Akt and is routinely used as a convenient indirect measure of Akt activation (21). Pancreatic acinar cells were treated with or without insulin in the absence or presence of LY294002 for 15 min. The cells were then lysed, and protein lysates were separated using SDS-PAGE and Western blotted using the pAktS473 antibody (Fig. 5, *top panel*). The pan-Akt antibody was used in parallel control experiments to determine whether equal amounts of protein (and specifically of Akt) were loaded into each lane (Fig. 5, *bottom panel*). Treatment with 100 nM insulin increased Akt phosphorylation, which was completely inhibited by co-incubation with the PI3K inhibitor, LY294002 (Fig. 5, *top panel*). In fact, LY294002 reduced Akt phosphorylation to well below control levels, suggesting that there may be some

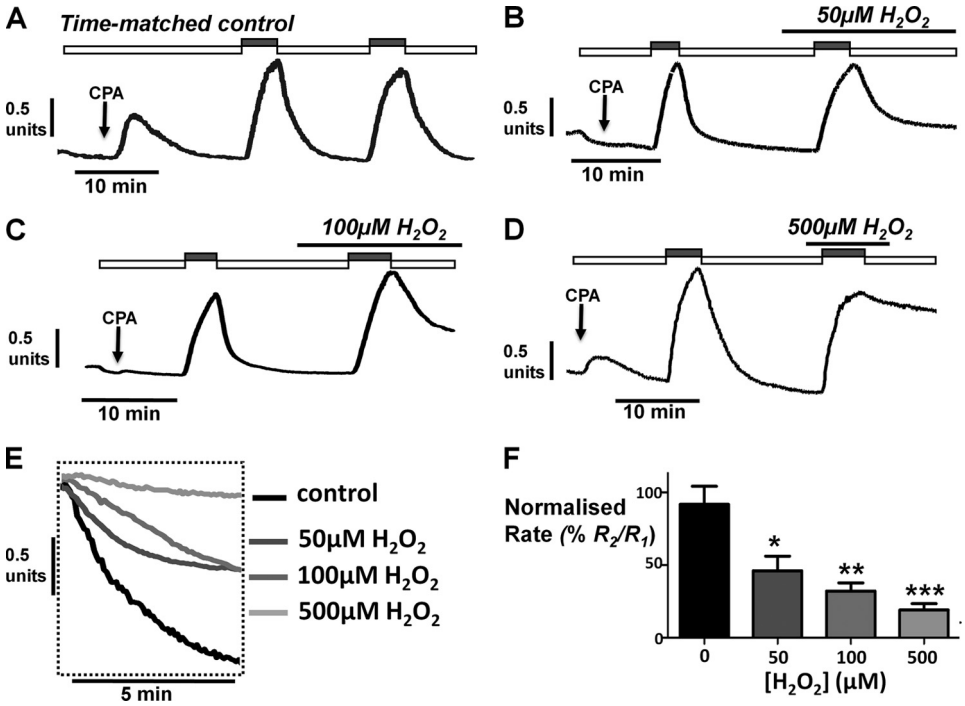

FIGURE 3. **H_2O_2 causes a concentration-dependent inhibition of PMCA activity in an *in situ* $[Ca^{2+}]_i$ clearance assay.** *A–D*, representative traces showing the *in situ* $[Ca^{2+}]_i$ clearance assay (see "Results") in untreated fura-2-loaded pancreatic acinar cells (time-matched control, $n = 8$; *A*) and cells treated with 50 μM H_2O_2 ($n = 4$, *B*), 100 μM H_2O_2 ($n = 6$, *C*), and 500 μM H_2O_2 ($n = 6$, *D*), during the second influx clearance challenge. The cells were treated with 30 μM cyclopiazonic acid (*CPA*, *arrow*) in the absence of external Ca^{2+} with 1 mM EGTA (*white box*) or 20 mM Ca^{2+} (*gray box*) to induce the Ca^{2+} influx phase. *E* shows expanded time courses taken from the second clearance phase in *A--D* in the presence of increasing concentrations of H_2O_2. Linear clearance rate (in the presence of H_2O_2) was normalized to the initial clearance rate in each cell (% relative clearance). *F*, mean percentage relative clearance (± S.E.). *, $p < 0.05$; **, $p < 0.01$; ***, $p < 0.001$, compared with time-matched control experiments (*black box*) as determined by a nonparametric Mann-Whitney *U* test.

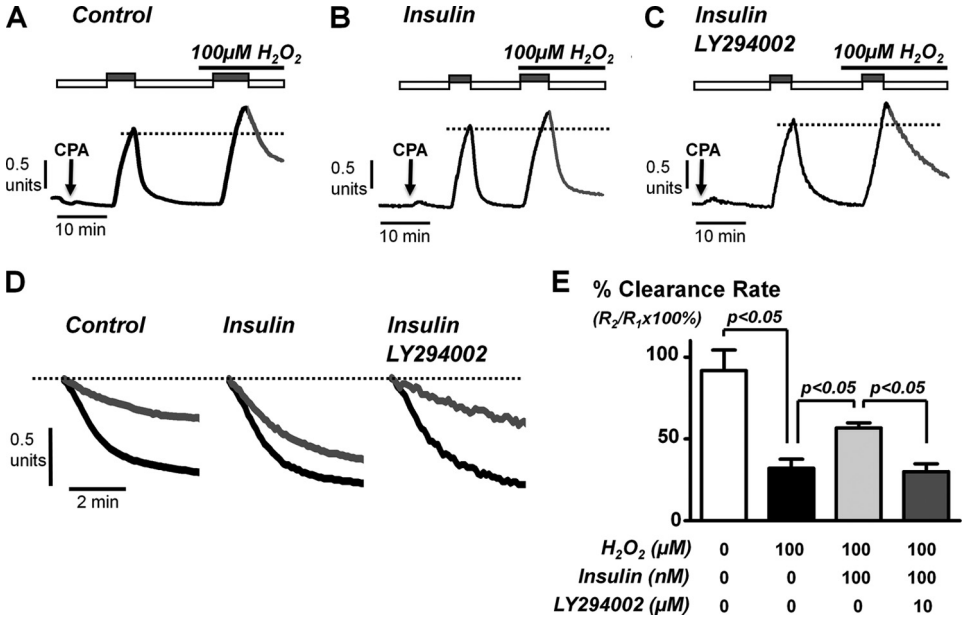

FIGURE 4. **Insulin protects the H_2O_2-induced inhibition of PMCA activity in a PI3K-dependent manner.** *A–C*, representative traces showing the *in situ* $[Ca^{2+}]_i$ clearance assay. Pancreatic acinar cells were treated with 100 μM H_2O_2 during the second influx-clearance challenge in untreated control cells ($n = 6$, *A*), cells pretreated with 100 nM insulin ($n = 6$, *B*), or a combination of insulin and LY294002 (10 μM) ($n = 5$, *C*) for 30 min. *D*, expanded time courses taken from traces in *A–C* comparing the initial control clearance (*black trace*) with clearance during treatment with 100 μM H_2O_2 (*gray traces*), measured from the same standardized value (*dotted line*). *E*, mean data (± S.E.) showing the effect of H_2O_2 on the percentage of relative clearance under the different treatment conditions. Statistical significance was $p < 0.05$ (*) as determined by a nonparametric Mann-Whitney *U* test. *CPA*, cyclopiazonic acid.

constitutive Akt phosphorylation in resting cells. However, the lack of effect of LY294002 on resting $[Ca^{2+}]_i$ suggests that reducing this constitutive Akt phosphorylation (with LY294002) has no effect on $[Ca^{2+}]_i$ homeostasis.

Insulin Has No Effect on H_2O_2-induced Mitochondrial Depolarization—A variety of evidence suggests that some of the major downstream targets of Akt reside at or within the mitochondria (26–28). Several of these molecular targets are

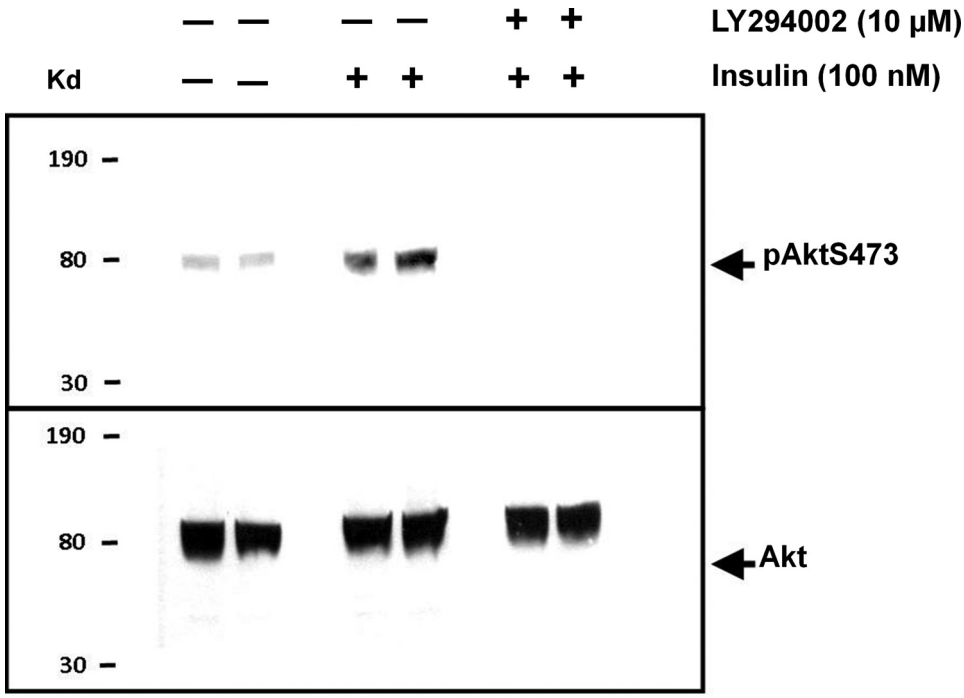

FIGURE 5. **Insulin induces AktS473 phosphorylation in a PI3K-dependent manner.** Representative Western blots using the pAktS473 antibody and pan-Akt antibody on cell lysates from pancreatic acinar treated with (+) or without (−) 100 nM insulin and/or 10 μM LY294002 for 15 min ($n = 4$). The pAktS473 antibody detects phosphorylated serine at position 473 on Akt, and the pan-Akt antibody was used as a loading control.

either components of or can regulate the activity of the mitochondrial permeability transition pore (mPTP). Our previous study showed that oxidant-induced inhibition of the PMCA coincided with mitochondrial depolarization and that both phenomena were prevented by inhibitors of the mPTP (5). This therefore suggested that the mechanism for the protective effect of insulin on Ca^{2+} overload and inhibition of the PMCA in pancreatic acinar cells might be due to protection of the mPTP and prevention of H_2O_2-induced mitochondrial depolarization. We tested this using TMRM to measure H_2O_2-induced mitochondrial depolarization. H_2O_2 induced a slow mitochondrial depolarization, whereas the protonophore and mitochondrial uncoupler, CCCP (4 μM), induced a rapid and almost complete mitochondrial depolarization (Fig. 6*A*). Surprisingly, H_2O_2 induced on average a 45 ± 6% (Fig. 6, *B* and *D*; $n = 6$ cells) depolarization in insulin-treated cells, which was indistinguishable from untreated control cells (51 ± 6%; $n = 6$ cells; Fig. 6, *A* and *D*). Moreover, insulin had no effect on TMRM fluorescence when applied to cells alone (Fig. 6, *C* and *D*). Collectively, these data suggest that protection against mitochondrial depolarization is unlikely to be the mechanism whereby insulin protects against oxidant-induced inhibition of the PMCA.

Insulin Attenuates the H_2O_2-induced ATP Depletion—Because insulin had no effect on mitochondrial depolarization, we next wanted to test whether insulin could protect against ATP depletion. This was investigated using two complimentary approaches; MgGreen fluorescence in intact living cells and *in vitro* chemiluminescence of firefly luciferase assays. MgGreen was used to assess ATP depletion indirectly by measuring free $[Mg^{2+}]$, as in our previous study (5). Using the MgGreen technique, 500 μM H_2O_2 caused 50 ± 3% ATP depletion (Fig. 7, *A* and *C*), consistent with our previous study (5). However, following treatment with 100 nM insulin, the response to 500 μM H_2O_2 was reduced to 15 ± 3% ATP depletion (Fig. 7, *B* and *C*).

For experiments using the *in vitro* firefly luciferase chemiluminescence ATP assays kits, the experimental design was essentially the same, except the cells were treated sequentially in suspension in Eppendorf tubes and centrifuged between treatments prior to cell lysis and assay of luminescence. A range of H_2O_2 concentrations were used to give a full H_2O_2 concentration-ATP depletion response curve in the absence or presence of insulin. These experiments revealed that H_2O_2 caused a steep concentration-dependent ATP depletion between 30 μM, at which there was no significant ATP depletion, and 300 μM, which reached close to maximum ATP depletion (Fig. 7*D*). The data were fitted to log transformed sigmoidal concentration-response curves, which generated an average IC_{50} of 86 ± 8 μM and Hill slope of 3.8 ± 1.3 ($n = 9$ assays, 5 rats; Fig. 7*D*, *filled square*). Pretreatment of cells with insulin (100 nM) caused a rightward shift in the concentration-response curve and significantly increased the average IC_{50} to 254 ± 42 μM ($p < 0.0001$; Hill slope of 2.7 ± 1.2; $n = 9$ assays, 5 rats; Fig. 7*D*, *open circle*). Surprisingly, insulin treatment alone (without H_2O_2) for the entire experimental period (3 × 20 min) had no significant effect on ATP levels compared with time-matched controls (105 ± 8%; $n = 9$ assays, 5 rats; Fig. 7*D*, *open triangle*). These data suggest that insulin protects acinar cells from substantial ATP depletion over a relatively narrow concentration range of H_2O_2.

Effect of Insulin on NAD(P)H Autofluorescence in Pancreatic Acinar Cells—To test whether insulin causes a metabolic switch from mitochondrial to predominantly glycolytic metabolism in pancreatic acinar cells, we next used NAD(P)H autofluorescence as an indirect measure of cellular metabolism. The major pool of cellular NAD(P)H is classically believed to be

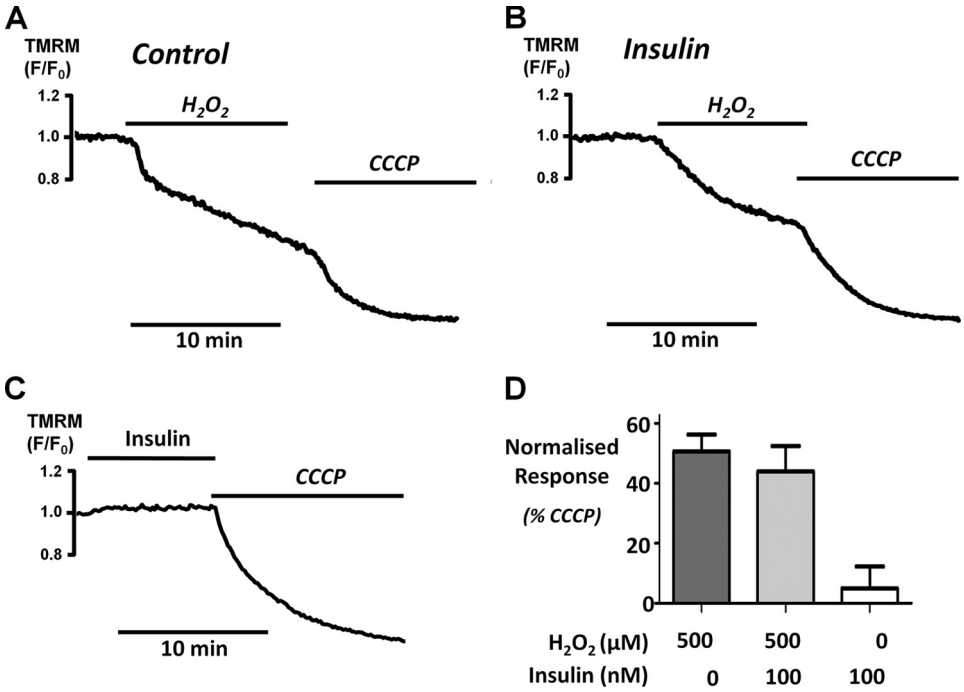

FIGURE 6. **Insulin has no effect on H_2O_2-induced depolarization of the mitochondrial membrane potential ($\Delta\Psi m$).** Representative traces showing the relative TMRM fluorescence (F/F_0) of cells treated with 500 μM H_2O_2 alone ($n = 6$, *A*) or in combination with 100 nM insulin ($n = 6$, *B*) or the effect of 100 nM insulin alone ($n = 4$, *C*). In all cases (*A–C*), 4 μM CCCP was added to the cells to induce a maximum depolarization as a positive control. *D*, the mean data were quantified and normalized by expressing the change in F/F_0 as a percentage of the CCCP response (*, $p < 0.05$, as assessed using a Mann-Whitney test).

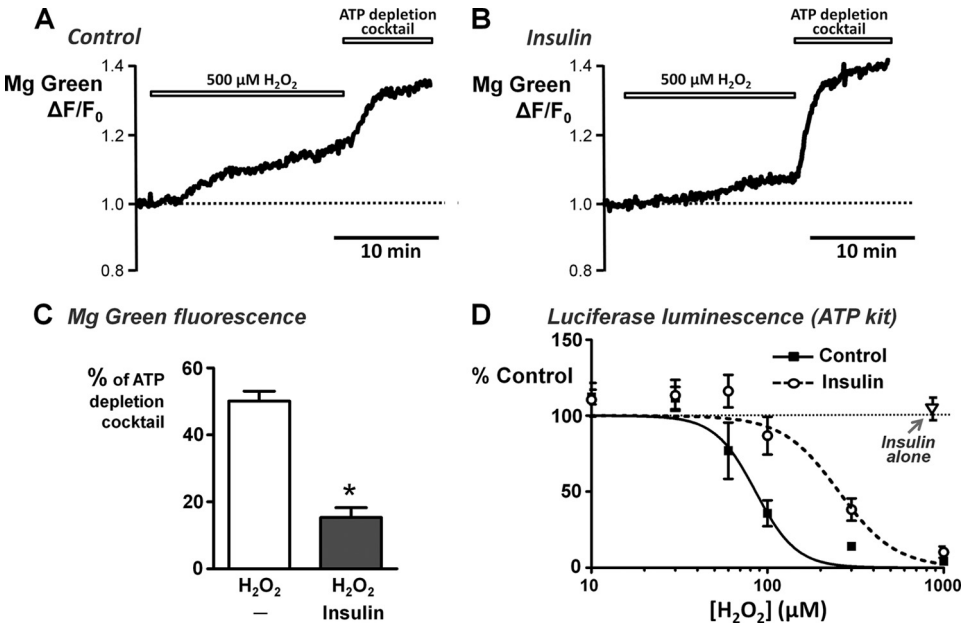

FIGURE 7. **Insulin attenuates H_2O_2-induced ATP depletion.** Cellular ATP was assessed using MgGreen fluorescence and the *in vitro* ViaLight® Plus luciferase-based chemiluminescence ATP monitoring kit. *A* and *B*, representative traces showing the relative MgGreen fluorescence (F/F_0) in response to 500 μM H_2O_2 followed by the "ATP depletion" mixture in untreated control cells (*A*) and cells pretreated with 100 nM insulin for 30 min (*B*). The ATP depletion mixture consisted of 100 μM CCh, 10 μM oligomycin, 2 mM iodoacetate, 500 μM bromopyruvate, and 4 μM CCCP to induce maximum ATP depletion. *C*, responses to H_2O_2 were quantified and normalized by expressing the change in F/F_0 as a percentage of the ATP depletion mixture response and compared between untreated control cells and insulin-treated cells (*, $p < 0.05$, as assessed using a Mann-Whitney *U* test). *D*, average H_2O_2 concentration-ATP depletion response curves for untreated control cells (*filled squares*) and cells pretreated with 100 nM insulin (*open circles*), measured using the ATP kit. Pancreatic acinar cells were treated with or without 100 nM insulin for 20 min, followed by treatment with or without various concentrations of H_2O_2 (0–1 mM) for a further 20 min. Luminescence of the "ATP-depletion mixture" (maximum ATP depletion) was subtracted prior to normalization to the corresponding time-matched control (total ATP). Additional control experiments were performed in which cells were treated with 100 nM insulin alone, without H_2O_2 (*open triangle*).

located within mitochondria, whereas a minor pool comes from glycolytic enzymes in the cytosol. Therefore to determine the relative contributions of mitochondrial *versus* cytosolic (glycolytic) NAD(P)H production, the cells were treated with CCCP (4 μM) to deplete mitochondrial NAD(P)H, followed by iodoacetate (IOA, 2 mM) to inhibit cytosolic (glycolytic) NAD(P)H

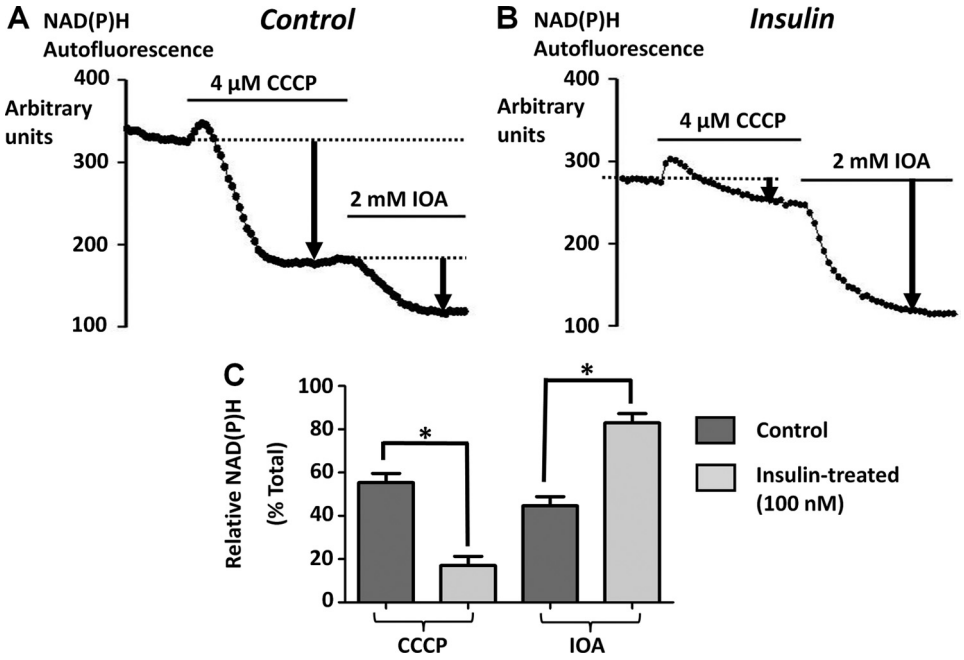

FIGURE 8. **Effect of insulin on the relative contributions of mitochondrial *versus* glycolytic NAD(P)H autofluorescence in pancreatic acinar cells.** The relative contributions of mitochondrial *versus* glycolytic NAD(P)H autofluorescence was determined by treating with 4 μM CCCP to deplete mitochondrial NAD(P)H and 2 mM IOA to inhibit glycolytic NAD(P)H production. *A* and *B*, representative traces of raw background-subtracted autofluorescence gray levels for untreated control cells ($n = 6$, *A*) and cells pretreated with 100 nM insulin ($n = 7$, *B*). The relative CCCP and iodoacetate-induced decrease in NAD(P)H autofluorescence was quantified and normalized by expressing as a percentage of the total decrease in NAD(P)H autofluorescence. *C*, mean data (± S.E.) for control and insulin-treated cells (*, $p < 0.05$, as assessed using a Mann-Whitney test).

production. The protonophore, CCCP, uncouples mitochondrial electron transport from ATP production by dissipating the electrochemical proton gradient, thereby allowing mitochondrial reducing equivalents (NAD(P)H) to be used up unproductively (29). IOA is a potent and irreversible inhibitor of glyceraldehyde phosphate dehydrogenase, which is the major glycolytic source of NADH (30). Therefore, the CCCP-induced decrease in NAD(P)H autofluorescence represents an indirect measure of mitochondrial metabolism; whereas the residual IOA-induced decrease in NAD(P)H autofluorescence represents an indirect measure of glycolytic metabolism. Similar methods have been used to assess the relative mitochondrial and glycolytic contribution to NADH production, and thus metabolism, in transformed hematopoietic cells (31). The relative CCCP- and IOA-induced changes in NAD(P)H autofluorescence were quantified and normalized by expressing them as a percentage of the total decrease in NAD(P)H autofluorescence (Fig. 8). In untreated control cells CCCP caused a 55 ± 4% decrease and IOA caused a 45 ± 4% decrease in NAD(P)H autofluorescence (Fig. 8, *A* and *C*; $n = 6$). However, in cells pretreated with 100 nM insulin for 30 min, the CCCP-induced decrease in NAD(P)H autofluorescence was markedly reduced to only 17 ± 4% (Fig. 8, *B* and *C*; $n = 7$, $p < 0.05$, assessed by Mann-Whitney test), whereas the IOA-induced decrease in NAD(P)H autofluorescence increased to 83 ± 4% (Fig. 8, *B* and *C*; $n = 7$, $p < 0.05$). These data suggest that insulin treatment switches pancreatic acinar cell metabolism from mitochondrial to predominantly glycolytic metabolism.

Insulin Potentiates the Inhibition of the PMCA by Glycolytic Inhibitors and Abolishes the Inhibition of the PMCA by Mitochondrial Inhibitors—Because of this insulin-induced metabolic switch, we reasoned that insulin may also affect the sensitivity of the PMCA to the glycolytic inhibitor, 3-bromopyruvate (BrPyr), *versus* the mitochondrial uncoupler, CCCP. BrPyr is an inhibitor of hexokinase, the first step in the glycolytic pathway. Similar to experiments performed in Fig. 4, the cells were treated with or without 100 nM insulin for 30 min prior to the start of the $[Ca^{2+}]_i$ clearance assay. Each metabolic inhibitor was then applied during the second clearance phase, and its effect was determined on the normalized clearance rate. In the absence of insulin treatment, BrPyr (500 μM) reduced $[Ca^{2+}]_i$ clearance to 45 ± 8% of the initial clearance rate ($n = 7$; Fig. 9, *A* and *E*) compared with time-matched control experiments (103 ± 3%, $n = 6$). However, in insulin-treated cells, the BrPyr-induced inhibition of $[Ca^{2+}]_i$ clearance was markedly potentiated to 12 ± 8% of the initial clearance rate ($n = 8$; Fig. 9, *B* and *E*; $p < 0.05$). Likewise CCCP (4 μM) decreased $[Ca^{2+}]_i$ clearance to 58 ± 10% of the of the initial clearance rate in untreated control cells ($n = 8$; Fig. 9, *C* and *E*), which was abolished to 115 ± 19% following insulin treatment ($n = 8$; Fig. 9, *D* and *E*). These data suggest that insulin treatment causes the PMCA to become almost entirely dependent on glycolysis as an ATP supply.

DISCUSSION

We have previously demonstrated that increased oxidative stress (H_2O_2) alters the normal pattern of CCK-evoked $[Ca^{2+}]_i$ signaling and impaired normal resting $[Ca^{2+}]_i$ homeostasis. This resulted in an irreversible increase in $[Ca^{2+}]_i$ (Ca^{2+} overload response) in an increasing proportion of cells with increasing concentration of H_2O_2 (6). The H_2O_2-induced Ca^{2+} overload we observed also corresponded to a marked inhibition of the PMCA (5). This inhibition is likely to be an important mechanism responsible for the irreversible nature of the Ca^{2+}

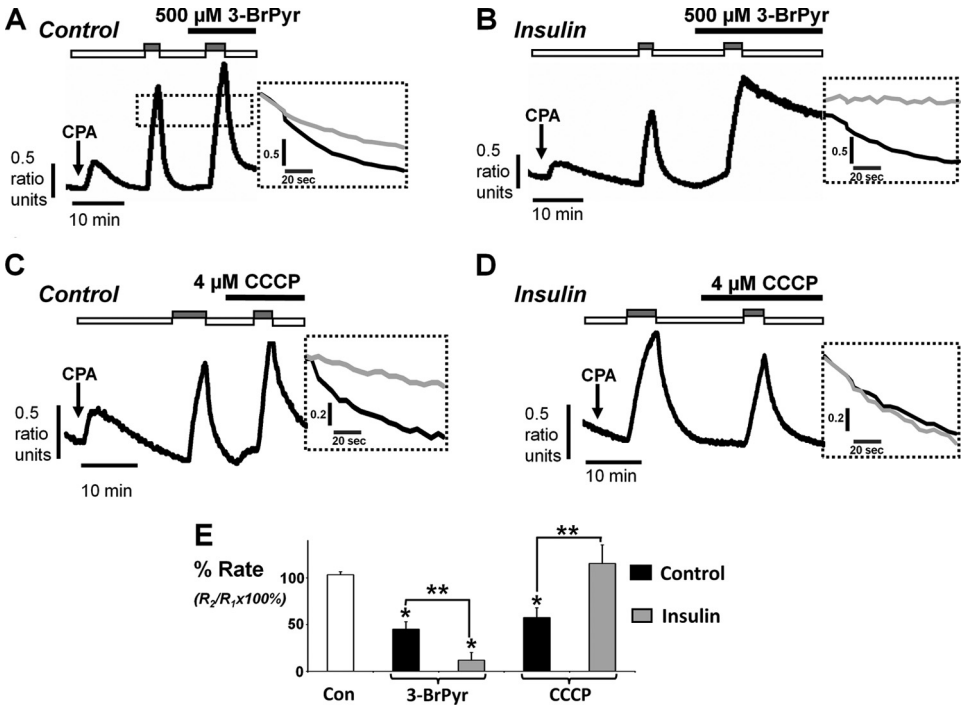

FIGURE 9. **Insulin potentiates BrPyr-induced inhibition of the PMCA and abolishes the CCCP-induced inhibition of the PMCA.** *A–D*, representative traces showing the *in situ* $[Ca^{2+}]_i$ clearance assay following treatment with metabolic inhibitors. Pancreatic acinar cells were treated with 500 μM BrPyr (*A* and *B*; $n =$ 7 and 8, respectively) or CCCP (*C* and *D*; $n = 8$ and 8, respectively) during the second influx clearance challenge in untreated control cells (*A* and *C*) or cells pretreated with 100 nM insulin for 30 min (*B* and *D*). Expanded time courses taken from each trace in *A*--*D* are shown in the adjacent *inset* comparing the initial control clearance (*black trace*) with clearance during metabolic inhibitor (*gray trace*) superimposed and measured from the same standardized value (*dotted line*). *E*, mean data (± S.E.) showing the effect of each metabolic inhibitor on the percentage of relative clearance in the absence and presence of insulin. The *white box* represents the time-matched controls, the *black* and *gray boxes* represent the effect of metabolic inhibitors on mean normalized Ca^{2+} clearance in untreated control cells and insulin-treated cells, respectively. Statistical significance was $p < 0.05$ (*) as determined by a nonparametric Mann-Whitney *U* test, compared with time-matched control and $p < 0.05$ (**), comparing between groups.

overload response because pancreatic acinar cells do not express Na^+-Ca^{2+} exchange or show functional Na^+-Ca^{2+} exchange activity (7) and the PMCA is thus the only Ca^{2+} efflux pathway. Even if other Ca^{2+} clearance pathways and $[Ca^{2+}]_i$ signaling are impaired, provided the PMCA remains functional, $[Ca^{2+}]_i$ will slowly recover. This can be seen, for instance, after cells are treated with inhibitors of sarco/endoplasmic reticulum Ca^{2+}-ATPase, such as cyclopiazonic acid. In the context of a cellular insult, as in pancreatitis, this gives the cell time to activate and up-regulate appropriate stress response pathways (32) or even allows the "safe dismantling" of the cell constituents by activation of apoptosis or autophagy (33).

The current study showed that the H_2O_2-induced Ca^{2+} overload response and inhibition of the PMCA was partially prevented by pretreatment with insulin. This functional protection by insulin was abolished by the PI3K inhibitor, LY294002, suggesting that the protection was due to activation of PI3K and was accompanied by Akt phosphorylation and thus activation. Protection by insulin was, however, independent of reduced oxidative stress or any protective effect of insulin on mitochondrial depolarization. Nevertheless, insulin attenuated the H_2O_2-induced ATP depletion, suggesting that treatment with insulin can maintain ATP despite impaired mitochondrial function. In addition, measurements of NAD(P)H autofluorescence revealed that insulin appeared to switch the mitochondrial metabolism toward a greater glycolytic contribution presumably sufficient to maintain ATP. Insulin also markedly potentiated the inhibition of the PMCA by glycolytic inhibitors yet abolished inhibition of the PMCA by mitochondrial inhibitors. This further suggests that this insulin-induced metabolic switch toward glycolysis is not only sufficient to maintain ATP but also makes the PMCA almost entirely dependent on glycolysis as the major ATP fuel. Therefore, even in the face of impaired mitochondrial function (*e.g.* following induction of pancreatitis by bile acids and fatty acid ethyl esters), insulin might be expected to enhance glycolytic ATP supply and thus maintain PMCA activity. This would help to prevent the cytotoxic Ca^{2+} overload and the consequent spiral of self-perpetuating tissue damage that occurs during pancreatitis.

As outlined in the introduction, there is substantial evidence from several unrelated experimental animal models of pancreatitis that insulin (10–13) and other growth factors/peptides (17–19) are protective. There is also a body of indirect circumstantial clinical evidence in humans that insulin offers some protection against pancreatitis, for example by reducing the mortality rate and reducing symptomatic pain (14–16). However, the data from the current study provide the first direct evidence that such protection occurs at the level of pancreatic acinar cells, a mechanism that could be exploited for the treatment of the disease.

Perhaps the simplest explanation for the protective effects of insulin is that insulin reduces intracellular oxidative stress. However, in the present study, insulin had no significant effect on H_2O_2-induced oxidative stress, as measured by DCF fluores-

cence, suggesting that increased cellular anti-oxidant capacity is unlikely to be responsible for the insulin protection.

Insulin activates a number of different signaling pathways, but perhaps the most widely studied is the activation of PI3K, the enzyme that converts phosphatidylinositol (4,5)-bisphosphate to phosphatidylinositol (3,4,5)-trisphosphate. Phosphatidylinositol (3,4,5)-trisphosphate recruits Akt to the plasma membrane, where it becomes activated by phosphorylation by phophoinositide-dependent kinase 1 (21). There is a body of evidence in a wide variety of cells and tissues that activation of Akt-dependent signaling pathways is largely cytoprotective (21). Nevertheless, and at apparent variance with this cytoprotective action of insulin and/or PI3K/Akt, there is also strong evidence that activation of the PI3K pathways can promote pancreatic damage in several unrelated experimental models of pancreatitis (34–37). Notably, pancreatic injury and clinical markers of pancreatitis were markedly reduced in mice in which the catalytic subunit (p110) of PI3Kγ was deleted (p110$\gamma^{-/-}$ mice) (35, 36). Moreover, the PI3K inhibitor LY294002 attenuated the bile-acid-induced Ca^{2+} overload responses and inhibition of sarco/endoplasmic reticulum Ca^{2+}-ATPase activity in isolated pancreatic acinar cells, suggesting that *activation* of the PI3K pathway was responsible for these bile acid effects (34, 38). However, the PI3K p110γ isoform, implicated in the above studies, has been suggested to facilitate inflammation (39) and is classically activated by G-protein-coupled receptors (*e.g.* CCK in caerulein pancreatitis), rather than by tyrosine kinase receptors that are activated by insulin (40). Furthermore, Akt is not thought to be the major downstream effector of PI3K p110γ (40). Low "physiological" concentrations of CCK (0.1 nM) have been shown to cause Akt phosphorylation in isolated pancreatic acinar cells, consistent with cytoprotection (41). This is supported by our previous study where H_2O_2 induced an irreversible Ca^{2+} overload in *fewer* acinar cells when the cells were treated with 20 pM CCK (6). However, high "cytotoxic" CCK concentrations (10–1000 nM) reduced Akt phosphorylation to below basal levels (41), consistent with inhibition of Akt, which is more likely to exacerbate acinar cell injury. In contrast to stimuli acting through GPCRs, insulin activates the class 1A PI3K p110α isoform (42). This PI3K isoform classically couples to the activation of Akt and caused marked Akt phosphorylation in pancreatic acinar cells (41) consistent with our current study. Notably, one of the earliest studies to implicate PI3K in pancreatitis suggested that caerulein activates class III PI3K, leading to an increase in phosphotidylinositol 3-phosphate, perturbation of Golgi stack-lysosome fusion, and the consequent intra-acinar trypsinogen activation (37). Therefore, we suggest that activation of *different* PI3K isoforms is likely to regulate diverse pathophysiological responses in pancreatic acinar cells, although activation of Akt is most likely to be cytoprotective.

The molecular mechanism for the protective effects of insulin and in particular the activation of PI3K/Akt pathways, on Ca^{2+} overload and inhibition of the PMCA in pancreatic acinar cells is likely to be complex, because PI3K/Akt couples to many downstream signaling pathways. These include increased cellular metabolism, cell proliferation, anti-apoptotic, and pro-survival pathways (21). However, because the protective effects of insulin that we observed were relatively short term (15–30 min), they are unlikely to be due to increased transcription or expression but rather suggest a rapid effect of post-translational signaling pathways, for example because of Akt phosphorylation.

Our data clearly demonstrate that insulin protects against oxidant-induced inhibition of PMCA activity. Interestingly, insulin and IGF-1 have been reported to increase PMCA activity in kidney proximal tubule basolateral membranes (43). This insulin-induced increase in PMCA activity was abolished in streptozocin-induced diabetic rats (43) obese fa/fa rats (44) and ob/ob mice (45), most likely because of insulin resistance and a loss of insulin effectiveness. Similarly, brain synaptic PMCA activity has also been reported to be reduced in streptozocin-induced diabetic rats (46), an effect reversed by exogenously applied insulin (47). These data suggest that insulin, either endogenously released or exogenously applied, increases PMCA activity. However, our data showed that insulin had no direct effect on PMCA activity when applied alone (without H_2O_2) during the *in situ* $[Ca^{2+}]_i$ clearance assay or when applied to resting cells. The protective effects of insulin on PMCA activity in the present study thus appeared to be due to a reduction in oxidant-induced inhibition rather than a direct activation of the PMCA.

In our previous study H_2O_2-induced inhibition of the PMCA was independent of mitochondrial Ca^{2+} handling but coincided with mitochondrial depolarization and was attenuated by inhibitors of the mPTP, such as cyclosporine A and bonkgrekic acid (5). This led us to hypothesize that inhibition of the PMCA was due in part to H_2O_2-induced opening of mPTP and mitochondrial depolarization. Based on these observations, it might be hypothesized that insulin protected the PMCA by reducing the opening of the mPTP and preventing mitochondrial depolarization. Indeed, some of the major targets of Akt reside at or within the mitochondria, including the Bad-Bcl-2/Bcl-X_L complex and the voltage-dependent anion channel-hexokinase II (HK-II) complex (26–28). Both of these pathways regulate the mPTP and facilitate the complex reciprocal regulation of metabolism and pro-survival pathways. However, to our surprise, insulin had no effect on H_2O_2-induced mitochondrial depolarization in the current study, suggesting that the mPTP plays no role in the protective effects of insulin.

Also in our previous study (5), low concentrations of H_2O_2 (50 μM) had no detectable effect on ATP depletion (measured with MgGreen) yet caused mitochondrial depolarization and substantial inhibition of the PMCA. These data led us to conclude that inhibition of the PMCA appeared to be independent of ATP depletion—or more accurately, could occur prior to substantial ATP depletion—but rather was more dependent on mitochondrial membrane potential. We therefore speculated that perhaps this apparent "ATP depletion-independent" inhibition of the PMCA could be due to the release of some putative PMCA-inhibitory factor from the mitochondria, although to date we have no direct evidence for such a mechanism. It is also important to note that part of the H_2O_2-induced inhibition of the PMCA may be due to direct oxidation of either the PMCA and/or calmodulin, which would occur independently of any mitochondrial depolarization or ATP depletion.

In the present study, using the luminescence-based kit, H_2O_2 caused substantial ATP depletion over a narrow range of concentrations (30–300 μM). This appears to be contradictory to MgGreen experiments in which lower concentration had no effect (5), and 500 μM caused only 50% ATP depletion. This apparent discrepancy could be explained by the fact that the MgGreen technique selects for the very best cells likely to be the most resistant to ATP depletion within a cell population. The ATP kit, on the other hand, measures total ATP depletion across the entire population and therefore does not exclude those cells that are already dying and thus likely highly sensitive to ATP depletion.

Nevertheless, these new data reinstate ATP depletion as a mechanism potentially contributing to PMCA inhibition. More importantly, because insulin had no effect on oxidative stress or mitochondrial depolarization, protection of the PMCA by insulin is likely to be due to prevention of ATP depletion. In addition, the residual, insulin-insensitive inhibition of the PMCA was likely independent of ATP depletion and more likely caused by direct oxidation (or even the release of some putative mitochondrial PMCA inhibitory factor via the opening of the mPTP).

In the current study, the changes in NADH autofluorescence suggest that insulin "switches" cellular metabolism from predominantly mitochondrial to glycolytic metabolism, which likely serves to maintain ATP supply to the PMCA in the face of oxidant-impaired mitochondrial function. In fact, insulin treatment caused the PMCA to become exquisitely sensitive to glycolytic inhibitors, suggesting that insulin caused the PMCA to become almost entirely dependent on glycolysis as an ATP supply. Such a metabolic switch, referred to as the "Warburg effect" after its discovery by Otto Warburg almost 90 years ago, is well documented to occur during cancer (48). In particular, PI3K and Akt are well documented to be constitutively up-regulated in cancer and have been suggested to play a major role in contributing to the metabolic phenotype of cancer cells (49). However, this Warburg effect is due to altered expression of metabolic enzymes and/or the signaling pathways that control these metabolic pathways (50) and thus is unlikely to explain the acute insulin-induced "metabolic switch" observed over the short time frame of our NAD(P)H experiments. Nonetheless, PI3K/Akt is one of the major downstream signaling pathways activated by insulin; therefore it is reasonable to suggest that the acute effects of insulin treatment can lead to the post-translation regulation of metabolism and thus mimic a short term metabolic phenotype of cancer cells.

There is substantial evidence that insulin and activation of PI3K/Akt increase glycolytic flux by activation of several steps of the glycolytic pathway. In particular, glycolytic flux is primarily regulated by the activity of phosphofructokinase-1, which catalyzes the conversion of fructose-6-phosphate to fructose-1,6-bisphosphate and represents the first irreversible and committed step in glycolysis. Insulin has been shown to directly activate phosphofructokinase-2 via Akt-mediated phosphorylation, which catalyzes the conversion of fructose-6-phosphate to fructose-2,6-bisphosphate, the most potent allosteric activator of phosphofructokinase-1 (51). Despite this, evidence suggests that insulin and activation of PI3K/Akt can increase both mitochondrial oxidative phosphorylation and glycolytic metabolism (27). This is difficult to reconcile the insulin-induced decrease in "mitochondrial" NAD(P)H observed in the current study. Nevertheless, studies have shown that Akt can increase NAD(P)H, lactate, and glucose consumption without affecting mitochondrial oxidative phosphorylation (52). Moreover, because of its anabolic nature, insulin not only increases glucose uptake and glycolytic flux but can also divert metabolic flux away from mitochondrial oxidative phosphorylation and toward fatty acid synthesis, glycogenesis, and the pentose phosphate pathway. In particular, insulin is reported to activate pyruvate dehydrogenase, ATP-citrate lyase and acetyl Co-A carboxylase, important regulatory steps that drive citrate from the Krebs cycle toward fatty acid synthesis (53–55). Collectively, these studies are broadly in line with our observation that insulin reduces the relative "mitochondrial" NAD(P)H and increases "glycolytic" NAD(P)H.

The notion that insulin switches metabolism from predominantly mitochondrial to glycoclytic metabolism may be extremely relevant in light of the published evidence that the PMCA has its own glycolytic ATP supply that may render it largely insensitive to inhibition of mitochondrial metabolism (56–58). Specifically, in isolated inside-out plasma membrane vesicles from pig stomach smooth muscle enriched with PMCA, an endogenous membrane-bound glycolytic system provided ATP to fuel the PMCA-dependent Ca^{2+} uptake (56, 57). Moreover, providing glycolytic *substrates* were present, the Ca^{2+} uptake (PMCA activity) persisted in the absence of an exogenously applied ATP-regenerating system (56, 57). These studies suggest that key glycolytic enzymes may provide the PMCA with a "privileged" source of ATP to fuel the PMCA. Under physiological conditions, when the bulk cytosolic ATP concentration is saturating for the PMCA (*i.e.* >1 mM), such close functional coupling between glycolytic enzymes and the PMCA is likely to be of minimal functional significance. In other words, the PMCA does not care where the ATP comes from: a mitochondrial source or glycolytic source. In fact it is likely that the majority of cytosolic ATP will come from mitochondria rather than glycolysis. However, in the face of impaired mitochondrial metabolism, for example under conditions of cellular stress, perhaps a glycolytic source of ATP—or more specifically an insulin-mediated "up-regulated" glycolytic source of ATP—is likely to be critical in maintaining PMCA activity and thus restoring low resting cytosolic $[Ca^{2+}]_i$. Under these stressed conditions, such a "privileged" source of ATP may be sufficient to "fuel" the PMCA, even if bulk (global) ATP is close to zero.

Collectively these data suggest that insulin protects the PMCA from oxidant-induced inhibition and the consequent Ca^{2+} overload by effectively redirecting ATP production from mitochondrial metabolism to glycolytic metabolism, which then fuels the PMCA in the face of impaired mitochondrial function. Such a mechanism may be very important in preventing pancreatic acinar cells from undergoing necrotic cell death during severe metabolic stress, such as when exposed to agents that induce pancreatitis. As such, we suggest that this mechanism is potentially of considerable pathophysiological importance.

Acknowledgment—We thank Prof. Mark Dunne for use of the BioTek Synergy HT luminescent multi-plate reader.

REFERENCES

1. Pandol, S. J., Saluja, A. K., Imrie, C. W., and Banks, P. A. (2007) Acute pancreatitis: bench to the bedside. *Gastroenterology* **132,** 1127–1151
2. Petersen, O. H., Tepikin, A. V., Gerasimenko, J. V., Gerasimenko, O. V., Sutton, R., and Criddle, D. N. (2009) Fatty acids, alcohol and fatty acid ethyl esters: toxic Ca^{2+} signal generation and pancreatitis. *Cell Calcium* **45,** 634–642
3. Suzuki, H., Suematsu, M., Miura, S., Asako, H., Kurose, I., Ishii, H., Houzawa, S., and Tsuchiya, M. (1993) Xanthine oxidase-mediated intracellular oxidative stress in response to cerulein in rat pancreatic acinar cells. *Pancreas* **8,** 465–470
4. Weber, C. K., and Adler, G. (2001) From acinar cell damage to systemic inflammatory response: current concepts in pancreatitis. *Pancreatology* **1,** 356–362
5. Baggaley, E. M., Elliott, A. C., and Bruce, J. I. (2008) Oxidant-induced inhibition of the plasma membrane Ca^{2+}-ATPase in pancreatic acinar cells: role of the mitochondria. *Am. J. Physiol. Cell Physiol.* **295,** C1247–C1260
6. Bruce, J. I., and Elliott, A. C. (2007) Oxidant-impaired intracellular Ca^{2+} signaling in pancreatic acinar cells: role of the plasma membrane Ca^{2+}-ATPase. *Am. J. Physiol. Cell Physiol.* **293,** C938–C950
7. Muallem, S., Beeker, T., and Pandol, S. J. (1988) Role of Na^{+}/Ca^{2+} exchange and the plasma membrane Ca^{2+} pump in hormone-mediated Ca^{2+} efflux from pancreatic acini. *J. Membr. Biol.* **102,** 153–162
8. Bruce, J. I. (2010) Plasma membrane calcium pump regulation by metabolic stress. *World J. Biol. Chem.* **1,** 221–228
9. Gukovskaya, A. S., Mareninova, O. A., Odinokova, I. V., Sung, K. F., Lugea, A., Fischer, L., Wang, Y. L., Gukovsky, I., and Pandol, S. J. (2006) *J. Gastroenterol. Hepatol.* **21,** (Suppl. 3) S10–S13
10. Hegyi, P., Rakonczay, Z., Jr., Sári, R., Góg, C., Lonovics, J., Takács, T., and Czakó, L. (2004) L-Arginine-induced experimental pancreatitis. *World J. Gastroenterol.* **10,** 2003–2009
11. Hegyi, P., Rakonczay-Jr, Z., Sari, R., Czako, L., Farkas, N., Gog, C., Nemeth, J., Lonovics, J., and Takacs, T. (2004) Insulin is necessary for the hypertrophic effect of cholecystokinin-octapeptide following acute necrotizing experimental pancreatitis. *World J. Gastroenterol.* **10,** 2275–2277
12. Hegyi, P., Takacs, T., Tiszlavicz, L., Czako, L., and Lonovics, J. (2000) Recovery of exocrine pancreas six months following pancreatitis induction with L-arginine in streptozotocin-diabetic rats. *J. Physiol.* **94,** 51–55
13. Takács, T., Hegyi, P., Jármay, K., Czakó, L., Góg, C., Rakonczay, Z., Jr., Németh, J., and Lonovics, J. (2001) Cholecystokinin fails to promote pancreatic regeneration in diabetic rats following the induction of experimental pancreatitis. *Pharmacol. Res.* **44,** 363–372
14. Hallberg, D. (1977) Acute pancreatitis treated with and without addition of insulin. *Acta Chir. Scand.* **143,** 451–456
15. Svensson, J. O. (1975) Role of intravenously infused insulin in treatment of acute pancreatitis: a double-blind study. *Scand. J. Gastroenterol.* **10,** 487–490
16. Tsuang, W., Navaneethan, U., Ruiz, L., Palascak, J. B., and Gelrud, A. (2009) Hypertriglyceridemic pancreatitis: presentation and management. *Am. J. Gastroenterol.* **104,** 984–991
17. Dembiński, A., Warzecha, Z., Ceranowicz, P., Cieszkowski, J., Pawlik, W. W., Tomaszewska, R., Kunierz-Cabala, B., Naskalski, J. W., Kuwahara, A., and Kato, I. (2006) Role of growth hormone and insulin-like growth factor-1 in the protective effect of ghrelin in ischemia/reperfusion-induced acute pancreatitis. *Growth Horm. IGF Res.* **16,** 348–356
18. Warzecha, Z., Dembinski, A., Ceranowicz, P., Konturek, S. J., Tomaszewska, R., Stachura, J., and Konturek, P. C. (2003) IGF-1 stimulates production of interleukin-10 and inhibits development of caerulein-induced pancreatitis. *J. Physiol. Pharmacol.* **54,** 575–590
19. Warzecha, Z., Dembiński, A., Konturek, P. C., Ceranowicz, P., Konturek, S. J., Tomaszewska, R., Schuppan, D., Stachura, J., and Nakamura, T. (2001) Hepatocyte growth factor attenuates pancreatic damage in caerulein-induced pancreatitis in rats. *Eur. J. Pharmacol.* **430,** 113–121
20. Dolado, I., and Nebreda, A. R. (2008) AKT and oxidative stress team up to kill cancer cells. *Cancer Cell* **14,** 427–429
21. Manning, B. D., and Cantley, L. C. (2007) AKT/PKB signaling: navigating downstream. *Cell* **129,** 1261–1274
22. Zhou, Y. J., Yang, H. W., Wang, X. G., and Zhang, H. (2009) Hepatocyte growth factor prevents advanced glycation end products-induced injury and oxidative stress through a PI3K/Akt-dependent pathway in human endothelial cells. *Life Sci.* **85,** 670–677
23. Corvera, S., Jaspers, S., and Pasceri, M. (1991) Acute inhibition of insulin-stimulated glucose transport by the phosphatase inhibitor, okadaic acid. *J. Biol. Chem.* **266,** 9271–9275
24. James, D. E., Brown, R., Navarro, J., and Pilch, P. F. (1988) Insulin-regulatable tissues express a unique insulin-sensitive glucose transport protein. *Nature* **333,** 183–185
25. Tanner, L. I., and Lienhard, G. E. (1987) Insulin elicits a redistribution of transferrin receptors in 3T3-L1 adipocytes through an increase in the rate constant for receptor externalization. *J. Biol. Chem.* **262,** 8975–8980
26. Majewski, N., Nogueira, V., Bhaskar, P., Coy, P. E., Skeen, J. E., Gottlob, K., Chandel, N. S., Thompson, C. B., Robey, R. B., and Hay, N. (2004) Hexokinase-mitochondria interaction mediated by Akt is required to inhibit apoptosis in the presence or absence of Bax and Bak. *Mol. Cell* **16,** 819–830
27. Miyamoto, S., Murphy, A. N., and Brown, J. H. (2008) Akt mediates mitochondrial protection in cardiomyocytes through phosphorylation of mitochondrial hexokinase-II. *Cell Death Differ.* **15,** 521–529
28. Pastorino, J. G., Hoek, J. B., and Shulga, N. (2005) Activation of glycogen synthase kinase 3β disrupts the binding of hexokinase II to mitochondria by phosphorylating voltage-dependent anion channel and potentiates chemotherapy-induced cytotoxicity. *Cancer Res.* **65,** 10545–10554
29. Duchen, M. R. (2000) Mitochondria and calcium: from cell signalling to cell death. *J. Physiol.* **529,** 57–68
30. Schmidt, M. M., and Dringen, R. (2009) Differential effects of iodoacetamide and iodoacetate on glycolysis and glutathione metabolism of cultured astrocytes. *Front. Neuroenergetics* **1,** 1
31. Rathmell, J. C., Fox, C. J., Plas, D. R., Hammerman, P. S., Cinalli, R. M., and Thompson, C. B. (2003) Akt-directed glucose metabolism can prevent Bax conformation change and promote growth factor-independent survival. *Mol. Cell Biol.* **23,** 7315–7328
32. Savkovi, V., Gaiser, S., Iovanna, J. L., and Bödeker, H. (2004) The stress response of the exocrine pancreas. *Dig. Dis.* **22,** 239–246
33. Odinokova, I. V., Sung, K. F., Mareninova, O. A., Hermann, K., Gukovsky, I., and Gukovskaya, A. S. (2008) Mitochondrial mechanisms of death responses in pancreatitis. *J. Gastroenterol. Hepatol.* **23** (Suppl. 1) S25–S30
34. Fischer, L., Gukovskaya, A. S., Young, S. H., Gukovsky, I., Lugea, A., Buechler, P., Penninger, J. M., Friess, H., and Pandol, S. J. (2004) Phosphatidylinositol 3-kinase regulates Ca^{2+} signaling in pancreatic acinar cells through inhibition of sarco(endo)plasmic reticulum Ca^{2+}-ATPase. *Am. J. Physiol. Gastrointest. Liver Physiol.* **287,** G1200–G1212
35. Gukovsky, I., Cheng, J. H., Nam, K. J., Lee, O. T., Lugea, A., Fischer, L., Penninger, J. M., Pandol, S. J., and Gukovskaya, A. S. (2004) Phosphatidylinositide 3-kinase γ regulates key pathologic responses to cholecystokinin in pancreatic acinar cells. *Gastroenterology* **126,** 554–566
36. Lupia, E., Goffi, A., De Giuli, P., Azzolino, O., Bosco, O., Patrucco, E., Vivaldo, M. C., Ricca, M., Wymann, M. P., Hirsch, E., Montrucchio, G., and Emanuelli, G. (2004) Ablation of phosphoinositide 3-kinase-γ reduces the severity of acute pancreatitis. *Am. J. Pathol.* **165,** 2003–2011
37. Singh, V. P., Saluja, A. K., Bhagat, L., van Acker, G. J., Song, A. M., Soltoff, S. P., Cantley, L. C., and Steer, M. L. (2001) Phosphatidylinositol 3-kinase-dependent activation of trypsinogen modulates the severity of acute pancreatitis. *J. Clin. Invest.* **108,** 1387–1395
38. Fischer, L., Gukovskaya, A. S., Penninger, J. M., Mareninova, O. A., Friess, H., Gukovsky, I., and Pandol, S. J. (2007) Phosphatidylinositol 3-kinase facilitates bile acid-induced Ca^{2+} responses in pancreatic acinar cells. *Am. J. Physiol. Gastrointest. Liver Physiol.* **292,** G875–G886
39. Wymann, M. P., Björklöf, K., Calvez, R., Finan, P., Thomast, M., Trifilieff, A., Barbier, M., Altruda, F., Hirsch, E., and Laffargue, M. (2003) Phosphoinositide 3-kinase γ: a key modulator in inflammation and allergy. *Biochem. Soc. Trans.* **31,** 275–280

40. Foster, F. M., Traer, C. J., Abraham, S. M., and Fry, M. J. (2003) The phosphoinositide (PI) 3-kinase family. *J. Cell Sci.* **116,** 3037–3040
41. Berna, M. J., Tapia, J. A., Sancho, V., Thill, M., Pace, A., Hoffmann, K. M., Gonzalez-Fernandez, L., and Jensen, R. T. (2009) Gastrointestinal growth factors and hormones have divergent effects on Akt activation. *Cell Signal.* **21,** 622–638
42. Wymann, M. P., Zvelebil, M., and Laffargue, M. (2003) Phosphoinositide 3-kinase signalling: which way to target? *Trends Pharmacol. Sci.* **24,** 366–376
43. Levy, J., Rempinski, D., and Kuo, T. H. (1994) Hormone-specific defect in insulin regulation of (Ca^{2+}/Mg^{2+})-adenosine triphosphatase activity in kidney membranes from streptozocin non-insulin-dependent diabetic rats. *Metabolism* **43,** 604–613
44. Levy, J., and Rempinski, D. (1994) Decreased activity of (Ca^{2+} + Mg^{2+})-adenosine triphosphatase (ATPase) and a hormone-specific defect in insulin regulation of ATPase in kidney basolateral membranes from obese fa/fa rats. *Metab. Clin Exp.* **43,** 1055–1061
45. Levy, J., and Gavin, J. R., 3rd. (1995) Different genes for obesity are associated with insulin loss of regulation of the membrane (Ca^{2+} + Mg^{2+})-ATPase in the obesity syndrome: lessons from animal models. *Int. J. Obes. Relat. Metab. Disord.* **19,** 97–102
46. Janicki, P. K., Horn, J. L., Singh, G., Franks, W. T., and Franks, J. J. (1994) Diminished brain synaptic plasma membrane Ca^{2+}-ATPase activity in rats with streptozocin-induced diabetes: association with reduced anesthetic requirements. *Life Sci.* **55,** PL359–PL364
47. Janicki, P. K., Horn, J. L., Singh, G., Janson, V. E., Franks, W. T., and Franks, J. J. (1995) Reduced anesthetic requirements, diminished brain plasma membrane Ca^{2+}-ATPase pumping, and enhanced brain synaptic plasma membrane phospholipid methylation in diabetic rats: effects of insulin. *Life Sci.* **56,** PL357–PL363
48. Warburg, O., Wind, F., and Negelein, E. (1927) The metabolism of tumors in the body. *J. Gen. Physiol.* **8,** 519–530
49. Wu, P., and Hu, Y. Z. (2010) PI3K/Akt/mTOR pathway inhibitors in cancer: a perspective on clinical progress. *Curr. Med. Chem.* **17,** 4326–4341
50. Pedersen, P. L. (2007) The cancer cell's "power plants" as promising therapeutic targets: an overview. *J. Bioenerg. Biomembr.* **39,** 1–12
51. Deprez, J., Vertommen, D., Alessi, D. R., Hue, L., and Rider, M. H. (1997) Phosphorylation and activation of heart 6-phosphofructo-2-kinase by protein kinase B and other protein kinases of the insulin signaling cascades. *J. Biol. Chem.* **272,** 17269–17275
52. Elstrom, R. L., Bauer, D. E., Buzzai, M., Karnauskas, R., Harris, M. H., Plas, D. R., Zhuang, H., Cinalli, R. M., Alavi, A., Rudin, C. M., and Thompson, C. B. (2004) Akt stimulates aerobic glycolysis in cancer cells. *Cancer Res.* **64,** 3892–3899
53. Berwick, D. C., Hers, I., Heesom, K. J., Moule, S. K., and Tavare, J. M. (2002) The identification of ATP-citrate lyase as a protein kinase B (Akt) substrate in primary adipocytes. *J. Biol. Chem.* **277,** 33895–33900
54. Borthwick, A. C., Edgell, N. J., and Denton, R. M. (1990) Protein-serine kinase from rat epididymal adipose tissue which phosphorylates and activates acetyl-CoA carboxylase: possible role in insulin action. *Biochem. J.* **270,** 795–801
55. Denton, R. M., McCormack, J. G., Rutter, G. A., Burnett, P., Edgell, N. J., Moule, S. K., and Diggle, T. A. (1996) The hormonal regulation of pyruvate dehydrogenase complex. *Adv. Enzyme Regul.* **36,** 183–198
56. Hardin, C. D., Raeymaekers, L., and Paul, R. J. (1992) Comparison of endogenous and exogenous sources of ATP in fueling Ca^{2+} uptake in smooth muscle plasma membrane vesicles. *J. Gen. Physiol.* **99,** 21–40
57. Hardin, C. D., Zhang, C., Kranias, E. G., Steenaart, N. A., Raeymaekers, L., and Paul, R. J. (1993) Regulation of glycolytically fueled Ca^{2+} uptake in smooth muscle plasmalemmal vesicles by phosphorylation. *Am. J. Physiol.* **265,** H1326–H1333
58. Paul, R. J., Hardin, C. D., Raeymaekers, L., Wuytack, F., and Casteels, R. (1989) Preferential support of Ca^{2+} uptake in smooth muscle plasma membrane vesicles by an endogenous glycolytic cascade. *FASEB J.* **3,** 2298–2301